Summer 6-12-2017

Structurally Diverse Boron-Nitrogen Heterocycles from an N2O23– Formazanate Ligand

Stephanie Barbon

Viktor Staroverov

Joe Gilroy
jgilroy5@uwo.ca

Structurally Diverse Boron-Nitrogen Heterocycles from an $N_2O_2^{3-}$ Formazanate Ligand

Stephanie M. Barbon,[a] Viktor N. Staroverov,[a] and Joe B. Gilroy*[a]

Abstract: Five new compounds comprised of unprecedented boron-nitrogen heterocycles have been isolated from a single reaction of a potentially tetradentate $N_2O_2^{3-}$ formazanate ligand with BF_3•OEt_2 and NEt_3. Optimized yields for each product were obtained through variation of experimental conditions and rationalized in terms of relative Gibbs free energies of the products as determined by electronic structure calculations. Chemical reduction of two of these compounds resulted in the formation of a stable anion, radical anion, and diradical dianion. Structural and electronic properties of this new family of redox-active heterocycles were characterized using UV-vis absorption spectroscopy, cyclic voltammetry and X-ray crystallography.

Boron-nitrogen (BN) heterocycles are of significant interest to a wide range of disciplines on account of their unusual structure, bonding, and properties.[1-3] The most common compounds containing such heterocycles, azaborines, find applications in organic electronics and chemical hydrogen storage.[4-6] Other BN heterocycles, exemplified by compounds **1**–**6**, are noted for their unexpected reactivity and, in many cases, unique redox properties.[7-16]

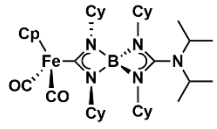

1 (Aldridge)

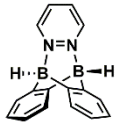

2 (Wagner)

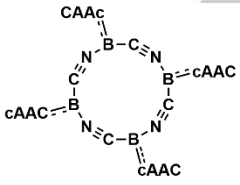

3 (Braunschweig)

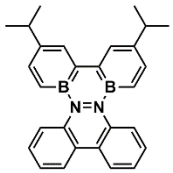

4 (Piers)

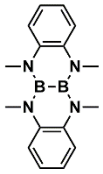

5 (Russell)

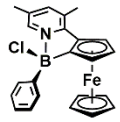

6 (Jäkle)

Each of compounds **1**–**3** contains BN bonds in an unusual framework.[17-19] Piers' B_2N_2 triphenylene analogue **4** can be reduced to form a stable radical anion,[20] and Russell's polycyclic borazine **5** undergoes oxidation to form a stable radical cation.[21] The Jäkle group has demonstrated that ferrocene-boron compound **6** can be converted to a planar borenium cation via abstraction of the chloride.[22]

[a] S. M. Barbon, Prof. Dr. V. N. Staroverov, Prof. Dr. J. B. Gilroy
Department of Chemistry and The Centre for Advanced Materials and Biomaterials Research (CAMBR)
The University of Western Ontario
1151 Richmond St. N., London, ON, Canada, N6A 5B7
E-mail: joe.gilroy@uwo.ca

Supporting information for this article is given via a link at the end of the document.

Our group is interested in boron complexes of formazanate ligands.[23] Boron difluoride adducts of these ligands have many fascinating and useful properties, including high molar absorptivities and a capacity for reversible stepwise reduction.[24-25] In this work, we set out to study the properties of similar compounds derived from trianionic, potentially tetradentate formazanate ligands.

The parent formazan **7** was synthesized according to a published method.[26] Upon reaction of **7** with BF_3•OEt_2 in the presence of NEt_3 followed by the addition of H_2O (Scheme 1), the expected product **8** was not detected; instead, the reaction mixture was found to contain formazan **7** and five new compounds (**9**–**13**), which could be separated by column chromatography in typical combined yields of 65–75% (Figure S1). Careful analysis of ^{1}H, ^{11}B, ^{13}C and ^{19}F NMR spectra, and single-crystal X-ray diffraction analysis enabled us to identify all six compounds present (Figures 1, 2, S2–S12). The complex reaction mixture obtained was in striking contrast to the clean conversion of formazan **14** to boron compound **15** in 92% yield under identical conditions (Scheme 1, Figures S13–S17).

To rationalize these observations, we used density-functional methods to calculate the changes in standard thermodynamic state functions for the reaction pathways leading from **7** to **8**–**13** and from **14** to **15** under the experimental reaction conditions (80 °C, 1 atm, toluene solution). The calculations were performed with the *Gaussian 09* program[27] using the hybrid version of the Perdew-Burke-Ernzerhof density functional[28] (PBE1PBE), the 6-311+G(d,p) basis set, and implicit solvation methods (Table S5). According to this level of theory, the formation of tetradentate boron compound **8** from **7** is thermodynamically unfavourable ($\Delta G°$ = 75.7 kJ mol^{-1}), whereas the formation of tetradentate compound **15** from **14** is favourable ($\Delta G°$ = −19.4 kJ mol^{-1}). It appears that the 5-membered chelates of **8** are too strained to form, so less strained compounds are produced instead. Compound **13**, the most abundant product which appears to form *via* **12**, was predicted to be decidedly favoured ($\Delta G°$ = −68.6 kJ mol^{-1}).

Through variation of reaction conditions, we optimized the yields of each of the five new compounds produced (Table S4). When elevated temperatures or longer reaction times were employed, the ratio of **13** to **9** and **10** was increased. When greater excess amounts of BF_3•OEt_2 and NEt_3 were used, products **9** and **10** were obtained in higher yields.

The six compounds present in the reaction mixture were separated by column chromatography (CH_2Cl_2, silica gel). The first two that eluted (R_f = 0.82, 0.76) yielded similar NMR spectra without ^{19}F resonances. We identified these compounds using X-ray crystallography as dimers **9** and **10** (Figure 1a, b). Both structures contain a ten-membered ring (-B-O-C-C-N-B-O-C-C-N-), where B–O bonds bridge the monomeric units. The difference between the two structures is the orientation of the ten-membered ring, a *pseudo*-chair conformation in compound **9** and a *pseudo*-boat conformation in compound **10** (see insets, Figure 1a, b). We did not observe interconversion between these two products in solution, even upon prolonged heating.

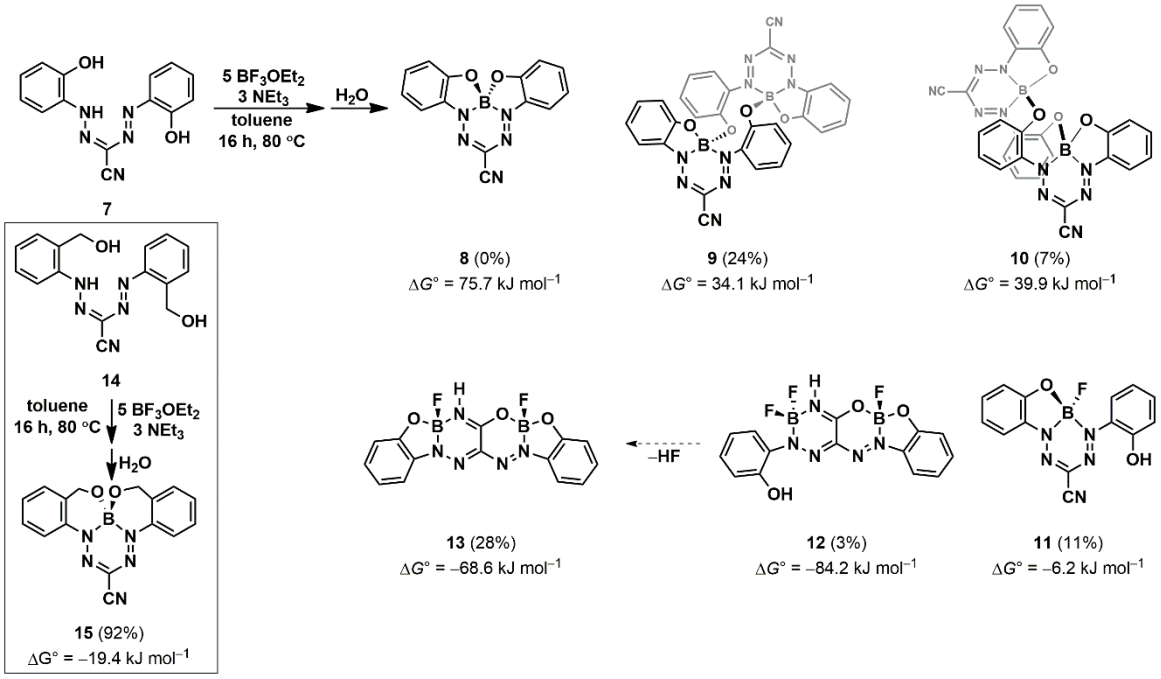

Scheme 1. Products formed from the reaction of formazan **7** with BF_3•OEt_2 and NEt_3. The inset indicates the product formed from the reaction of formazan **14** with BF_3•OEt_2 and NEt_3. The Gibbs free energies ($\Delta G°$) were computed for the formation of each compound from the corresponding formazan and the stoichiometric number of BF_3 and H_2O molecules under conditions simulating those employed in the actual synthesis, and are expressed in kJ mol^{-1} of the formazan. The dashed arrow indicates interconversion in solution.

The *pseudo*-boat conformation leads to a π-stacking interaction between aryl substituents and the formazanate backbone in the solid-state phase of **10**, which is not observed in **9**. In solution, this interaction causes broadening of the low-energy absorption of **10** and the appearance of a shoulder at 597 nm that is not present in the absorption profile of **9** (Figures 1e, S18, Table S1).

The cyclic voltammograms (CVs) of compounds **9** and **10** included three reduction waves (Figure 1f, Table S1). Both compounds exhibit two reversible one-electron reduction waves (**9**: E_{red1} = −760 mV, E_{red2} = −1010 mV; **10**: E_{red1} = −720 mV, E_{red2} = −1020 mV), and a third irreversible two-electron reduction (**9**: E_{onset} = −1730 mV; **10**: E_{onset} = −1770 mV). The reversible waves correspond to the stepwise reduction of the formazanate backbones to *mono*- and *bis*-radical anions and the irreversible wave to the formation of *bis*-dianions. The difference between the reversible reduction potentials (ΔE_{red}) was 250 mV for **9** and 290 mV for **10**.

Compound **10** proved easier to isolate than its structural isomer **9**, so it was chosen for further reactivity studies. Reduction with one and two equivalents of cobaltocene yielded compounds $\mathbf{10}^{\bullet-}$ and $\mathbf{10}^{\bullet 2-}$, both of which produced broad isotropic EPR spectra at g = 2.0038 (Figure S19). Both species were characterized by single-crystal X-ray diffraction analysis (Figure 1c, d, Table S2). The average N–N bond length in the neutral dimer **10** was 1.314(3) Å, which is typical of an N–N bond with a bond order of ~1.5. In compound $\mathbf{10}^{\bullet-}$, the average N–N bond length for N1 to N4 is 1.360(3) Å, suggesting the presence of a borataverdazyl radical in which the additional electron occupies an orbital with antibonding N–N character.[24, 29-30] The average N–N bond length for N5 to N8 is 1.315(3) Å, typical of a formazanate adduct.[24] These metrics confirm that chemical reduction occurs in a stepwise fashion and that the radical anion is localized on one formazanate ligand. In the doubly reduced species $\mathbf{10}^{\bullet 2-}$, the average N–N bond length was 1.366(3) Å, which corresponds to N–N single bonds as expected for borataverdazyl radicals.[30] These conclusions were corroborated by UV-vis absorption spectroscopy in CH_3CN (Figure 1e, Table S1). Neutral dimer **10** has a λ_{max} at 569 nm and a molar absorptivity (ε) of 20 500 M^{-1} cm^{-1}. Singly reduced $\mathbf{10}^{\bullet-}$ absorbs strongly at 568 nm, as well as 687 and 477 nm, which is typical of verdazyl species[30] and shows that $\mathbf{10}^{\bullet-}$ is made up of independent borataverdazyl and formazanate units. Doubly reduced species $\mathbf{10}^{\bullet 2-}$ absorbs minimally at 568 nm, but exhibits two absorption peaks typical of borataverdazyl anions with λ_{max} of 687 nm (ε = 8 200 M^{-1} cm^{-1}) and 477 nm (ε = 39 200 M^{-1} cm^{-1}).[31]

We were unable to grow single crystals of the third compound to elute (R_f = 0.61). However, using ^{1}H, ^{11}B, ^{13}C and ^{19}F NMR spectroscopy and mass spectrometry, we identified it as **11**. This product is dark blue, can be reversibly reduced twice (Figures S20, S21, Table S1), and slowly converts to formazan **7** in solution. The fourth compound that eluted from the column (R_f = 0.39) was formazan **7**, present as a result of incomplete reactivity or hydrolysis of unstable, unidentified species formed during the reaction.

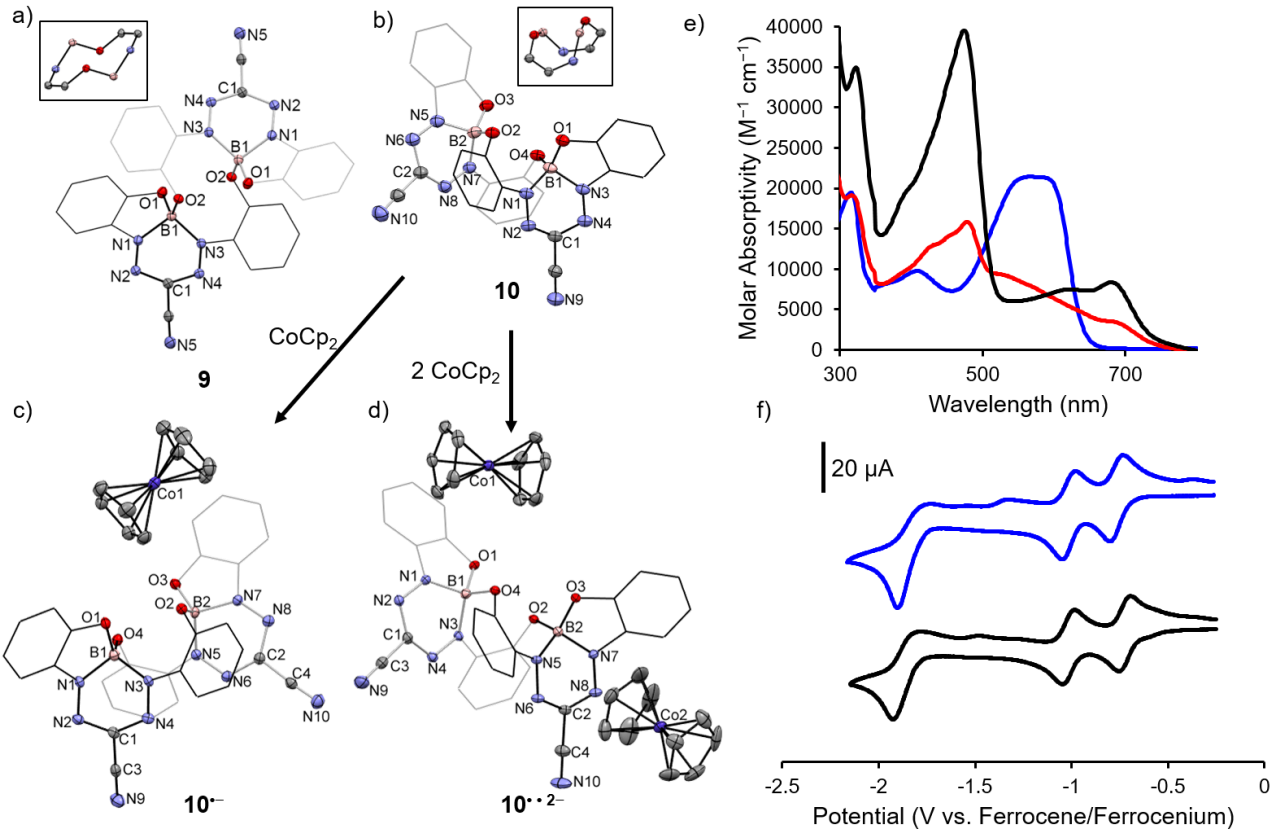

Figure 1. Solid-state structures of (a) **9**, (b) **10**, (c) **10**$^{\bullet-}$ and (d) **10**$^{\bullet\bullet 2-}$. Thermal displacement ellipsoids are shown at the 50% probability level. Phenyl substituents are wireframe and hydrogen atoms are removed for clarity. Arrows indicate conditions for the formation of **10**$^{-}$ and **10**$^{\bullet\bullet 2-}$. Insets in panels (a) and (b) show only the atoms in the respective ten-membered rings. Panel (e) shows UV-vis absorption spectra of compounds **10** (blue), **10**$^{\bullet-}$ (red) and **10**$^{\bullet\bullet 2-}$ (black) in CH_3CN. Panel (f) shows CVs of **9** (black) and **10** (blue) recorded at 100 mV s^{-1} in 1 mM CH_2Cl_2 solutions containing 0.1 M [nBu$_4$N][PF$_6$] as supporting electrolyte.

The final two compounds that eluted from the column (R_f = 0.31, 0.22) were identified as **12** and **13**. Interestingly, **13** showed two doublets in its ^{11}B NMR spectrum due to the coupling of each boron atom with a single fluorine atom ($^1J_{BF}$ = 33, 42 Hz). Single-crystal X-ray diffraction analysis confirmed that compound **13** was not a dimer, but contained two boron atoms bonded to one formazanate ligand, where the cyano group had been hydrolyzed.[32] Compound **12** is similar to **13** aside from a free OH group and a BF_2 unit. In solution, **12** converts to **13** over the course of a few hours. The λ_{max} of **12** is blue-shifted by 17 nm in CH_2Cl_2 with respect to **13** (Figure S22, S23). Compound **13** yielded a single reversible one-electron reduction in its CV (Figure S24), prompting us to perform chemical reduction using one equivalent of cobaltocene. The solution changed from pink-purple to dark blue-purple (Figure 2a). Attempts to crystallize the resulting compounds were unsuccessful, so a salt metathesis reaction was performed with [nBu$_4$N][Br] in order to exchange the cobaltocenium cation for the solubilizing tetra-*n*-butyl ammonium cation. The colour of the solution was unchanged throughout this process. Single-crystal X-ray diffraction revealed the resulting product to be anion **16**$^{-}$. Upon reduction, the NH bond in **13** appears to cleave homolytically, resulting in the formation of **16**$^{-}$ and H_2 (Figure 2c). The proposed structure was confirmed by ^{1}H and ^{13}C NMR spectroscopy, mass spectrometry and IR spectroscopy (see Figure S25, S26). Aside from the loss of the *N*-bonded proton, the connectivity in **16**$^{-}$ is identical to that of **13** (Figures 2b, c). The B1-N5 bond has shortened (**13**: 1.516(3) Å; **16**$^{-}$: 1.442(5) Å) and the C2-N5 bond has lengthened (**13**: 1.304(3) Å; **16**$^{-}$: 1.327(4) Å, Table 3). The angles around B1 and N5 change with the presence of the lone pair. For example, the N1-B1-N5 angle widens by ~3.5°, while the B1-N5-C2 angle contracts by ~3.6°. The same angles around B2 change less drastically (N3-B2-O2 angle contracts by 1.1°, and the B2-O3-C2 angle contracts by 2.0°). **16**$^{-}$ is highly absorbing (ε = 18 000 M^{-1} cm^{-1}), with a low-energy λ_{max} of 589 nm that was red-shifted by 12 nm with respect to neutral **13** (Figures S23, S27).

The calculated highest occupied molecular orbitals (HOMO) of **13** and **16**$^{-}$ are delocalized over the entire molecules (Figure 2d). The lowest unoccupied molecular orbitals (LUMO) were delocalized over the formazanate nitrogen atoms and the *N*-aryl substituents. Time-dependent PBE1PBE/6-311+G(d,p) calculations for **13** and **16**$^{-}$ in CH_2Cl_2 solution showed the HOMO and LUMO to be the dominant orbital pair involved in the lowest-energy electronic excitation in both molecules, and approximately reproduced the shift in λ_{max} from **13** to **16**$^{-}$ ($\Delta\lambda_{calc}$ = 8 nm, $\Delta\lambda_{obs}$ = 12 nm, Table S6).

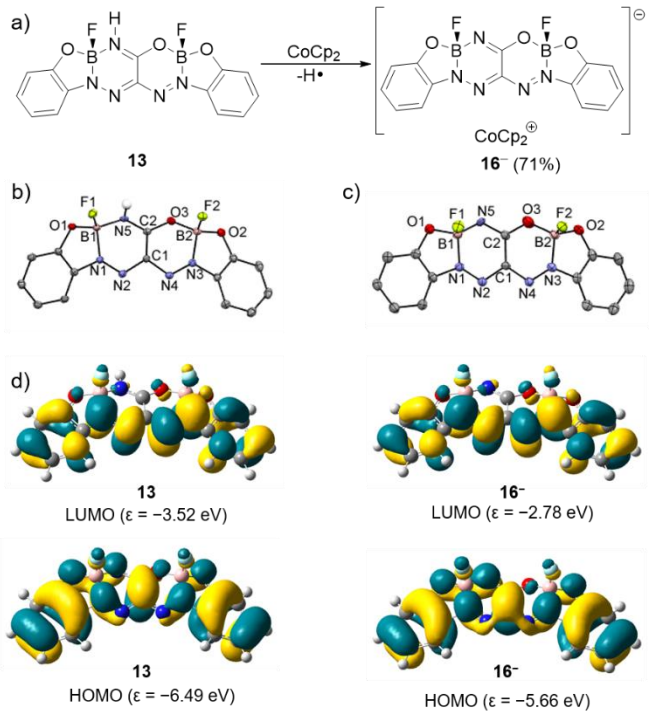

Figure 2. (a) Chemical reduction of **13** to **16**$^-$ with cobaltocene. Solid-state structures of (b) **13** and (c) **16**$^-$ with thermal displacement ellipsoids shown at the 50% probability level. Hydrogens, aside from the hydrogen on N5 in **13**, and the *n*Bu_4N cation in **16**$^-$ have been removed for clarity. (d) HOMOs and LUMOs for **13** and **16**$^-$ calculated at the PBE1PBE/6-311+G(d,p) level.

In conclusion, we have reported the synthesis of five new BN heterocycles **9**–**13** by one straightforward reaction, starting from an $N_2O_2^{3-}$ formazanate ligand. The observed product distribution appears to be strain-driven as evidenced by the fact that similar heterocycles were not formed when the reactant **7** was replaced by a homologous compound **14**. Each of compounds **9**–**13** exhibited interesting optical and electrochemical properties. In particular, compound **10** was reduced to stable *mono*- and *bis*-radical anions with electronically-isolated formazanate/verdazyl units. Compound **13**, which contains an unprecedented BN core, could be readily converted into stable anion **16**$^-$. This study will form a platform for the rational design of novel BN heterocycles with potential utility as light-harvesting and charge-transporting materials in the future.

Acknowledgements

This work was supported by the Natural Science and Engineering Research Council (NSERC) of Canada (J. B. G.: DG RGPIN-2013-435675, V. N. S.: DG RGPIN-2015-04814 and S. M. B.: CGS D scholarship), the Ontario Ministry of Research and Innovation (J. B. G.: ERA, ER-14-10-147) and the Canadian Foundation for Innovation (J. B. G.: JELF 33977).

Keywords: BN Heterocycles • Formazanate Ligands • Redox Chemistry • Boron Chemistry • Stable Radicals

[1] M. J. D. Bosdet and W. E. Piers, *Can. J. Chem.*, **2009**, *87*, 8–29.
[2] K. Ma, M. Scheibitz, S. Scholz and M. Wagner, *J. Organomet. Chem.*, **2002**, *652*, 11–19.
[3] J. Brand, H. Braunschweig and S. S. Sen, *Acc. Chem. Res.*, **2014**, *47*, 180–191.
[4] P. G. Campbell, A. J. V. Marwitz and S.-Y. Liu, *Angew. Chem. Int. Ed.*, **2012**, *51*, 6074–6092.
[5] P. G. Campbell, L. N. Zakharov, D. J. Grant, D. A. Dixon and S.-Y. Liu, *J. Am. Chem. Soc.*, **2010**, *132*, 3289–3291.
[6] X.-Y. Wang, H.-R. Lin, T. Lei, D.-C. Yang, F.-D. Zhuang, J.-Y. Wang, S.-C. Yuan and J. Pei, *Angew. Chem. Int. Ed.*, **2013**, *52*, 3117–3120.
[7] J. S. A. Ishibashi, J. L. Marshall, A. Mazière, G. J. Lovinger, B. Li, L. N. Zakharov, A. Dargelos, A. Graciaa, A. Chrostowska and S.-Y. Liu, *J. Am. Chem. Soc.*, **2014**, *136*, 15414–15421.
[8] H. Braunschweig, W. C. Ewing, K. Geetharani and M. Schäfer, *Angew. Chem. Int. Ed.*, **2015**, *54*, 1662–1665.
[9] D.-T. Yang, S. K. Mellerup, J.-B. Peng, X. Wang, Q.-S. Li and S. Wang, *J. Am. Chem. Soc.*, **2016**, *138*, 11513–11516.
[10] O. Dilek, Z. Lei, K. Mukherjee and S. Bane, *Chem. Commun.*, **2015**, *51*, 16992–16995.
[11] H. Braunschweig, T. Herbst, D. Rais, S. Ghosh, T. Kupfer, K. Radacki, A. G. Crawford, R. M. Ward, T. B. Marder, I. Fernández and G. Frenking, *J. Am. Chem. Soc.*, **2009**, *131*, 8989–8999.
[12] S. Pietsch, U. Paul, I. A. Cade, M. J. Ingleson, U. Radius and T. B. Marder, *Chem. Eur. J.*, **2015**, *21*, 9018–9021.
[13] A. W. Baggett, F. Guo, B. Li, S.-Y. Liu and F. Jäkle, *Angew. Chem. Int. Ed.*, **2015**, *54*, 11191–11195.
[14] H. Noda, M. Furutachi, Y. Asada, M. Shibasaki and N. Kumagai, *Nat. Chem.*, **2017**, DOI: 10.1038/nchem.2708.
[15] H. Helten, *Chem. Eur. J.*, **2016**, *22*, 12972–12982.
[16] M.-C. Chang and E. Otten, *Inorg. Chem.*, **2015**, *54*, 8656–8664.
[17] G. A. Pierce, S. Aldridge, C. Jones, T. Gans-Eichler, A. Stasch, N. D. Coombs and D. J. Willock, *Angew. Chem. Int. Ed.*, **2007**, *46*, 2043–2046.
[18] A. Lorbach, M. Bolte, H.-W. Lerner and M. Wagner, *Chem. Commun.*, **2010**, *46*, 3592–3594.
[19] M. Arrowsmith, D. Auerhammer, R. Bertermann, H. Braunschweig, G. Bringmann, M. A. Celik, R. D. Dewhurst, M. Finze, M. Grüne, M. Hailmann, T. Hertle and I. Krummenacher, *Angew. Chem. Int. Ed.*, **2016**, *55*, 14464–14468.
[20] C. A. Jaska, D. J. H. Emslie, M. J. D. Bosdet, W. E. Piers, T. S. Sorensen and M. Parvez, *J. Am. Chem. Soc.*, **2006**, *128*, 10885–10896.
[21] X. Xie, C. J. Adams, M. A. M. Al-Ibadi, J. E. McGrady, N. C. Norman and C. A. Russell, *Chem. Commun.*, **2013**, *49*, 10364–10366.
[22] J. Chen, R. A. Lalancette and F. Jäkle, *Chem. Commun.*, **2013**, *49*, 4893–4895.
[23] A. W. Nineham, *Chem. Rev.*, **1955**, *55*, 355–483.
[24] S. M. Barbon, P. A. Reinkeluers, J. T. Price, V. N. Staroverov and J. B. Gilroy, *Chem. Eur. J.*, **2014**, *20*, 11340–11344.
[25] M.-C. Chang and E. Otten, *Chem. Commun.*, **2014**, *50*, 7431–7433.
[26] J. B. Gilroy, P. O. Otieno, M. J. Ferguson, R. McDonald and R. G. Hicks, *Inorg. Chem.*, **2008**, *47*, 1279–1286.
[27] M. J. Frisch, G. W. Trucks, H. B. Schlegel *et al.*, Gaussian 09, Revision E.01 (Gaussian, Inc., Wallingford CT, 2013).
[28] M. Ernzerhof and G. E. Scuseria, *J. Chem. Phys.*, **1999**, *110*, 5029–5036.
[29] J. B. Gilroy, M. J. Ferguson, R. McDonald, B. O. Patrick and R. G. Hicks, *Chem. Commun.*, **2007**, 126–128.
[30] M.-C. Chang, A. Chantzis, D. Jacquemin and E. Otten, *Dalton Trans.*, **2016**, *45*, 9477–9484.
[31] The contribution from cobaltocenium is assumed to be negligible above 300 nm. See N. El Murr, *J. Organomet. Chem.*, **1976**, *112*, 189–199.
[32] Quenching the reaction with ammonia did not afford the symmetric analog of **13**.

Entry for the Table of Contents

COMMUNICATION

Five novel boron-nitrogen heterocycles based on an $N_2O_2^{3-}$ formazanate ligand have been isolated as unexpected products of a single reaction. The reduction of two of these heterocycles yielded an unusual anion, radical anion, and diradical dianion.

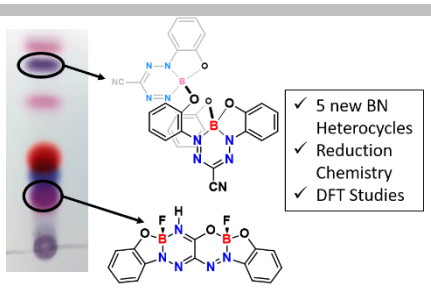

*S. M. Barbon, V. N. Staroverov, J. B. Gilroy**

Page No. – Page No.

Structurally Diverse Boron-Nitrogen Heterocycles from an $N_2O_2^{3-}$ Formazanate Ligand